PROGRESS IN NON-DESTRUCTIVE FATIGUE CRACK DETECTION AND MONITORING IN WELDED PRESSURE VESSELS SUBJECTED TO EXTERNAL PRESSURE CYCLING*

I.M. Kilpatrick
Principal Scientific Officer
Admiralty Marine
Technology Establishment
Dunfermline, Scotland

J.M. Cargill
Senior Scientific Officer
Admiralty Marine
Technology Establishment
Dunfermline, Scotland

INTRODUCTION

At the 1980 Review of Progress in Quantitative NDE the authors presented a paper outlining the NDE techniques then under development for fatigue crack detection and monitoring in welded structures (1). The present paper describes the progress made since then in applying the techniques to welded pressure vessels.

AMTE (Dunfermline) is concerned with the fatigue performance of externally pressurised vessels. In general these are internal ring-frame stiffened cylinders, Fig. 1 shows a typical structure.

Under compressive loading, fatigue cracking would not normally be expected to occur. However, the vessels are fabricated by welding. This sets up tensile residual stresses which are especially important at the stiffener to shell T-butt welds where cracking is expected to start. Thus the applied compressive cyclic load superimposed on a tensile residual stress results in a net tension cycle under which fatigue cracks can grow.

Results are presented from a fatigue test on a simple cylindrical vessel, stiffened internally by a deep bulkhead. The results illustrate the important part played by NDE in enabling data on crack initiation and propagation to be obtained, and how such experimental data compares with a fracture mechanics based fatigue analysis of the structure.

On-line underwater monitoring of fatigue crack growth is also described.

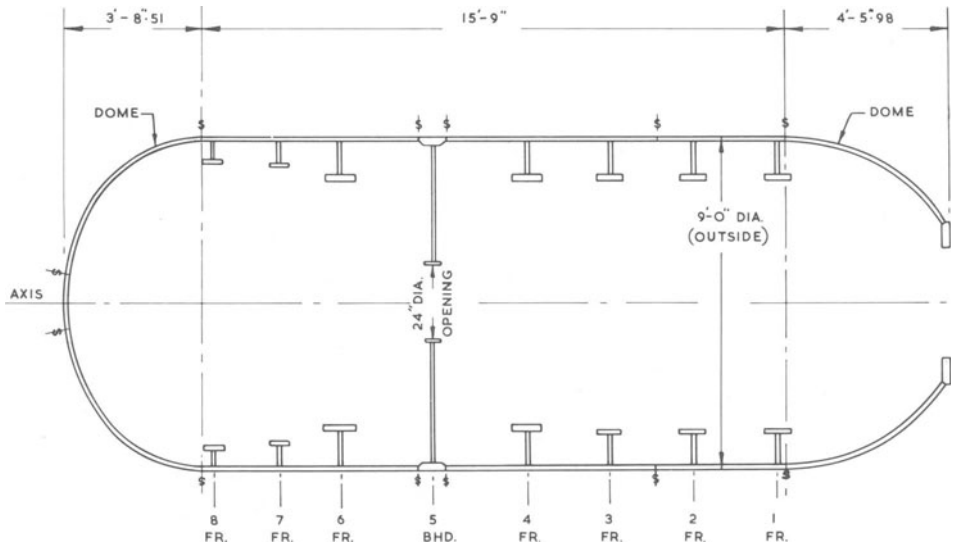

Fig. 1. Typical Internally Ring-frame Stiffened Vessel.

RESULTS OF A FATIGUE TEST ON AN INTERNALLY STIFFENED SIMPLE CYLINDER VESSEL - S8/1

Fig. 2 shows the vessel tested. This was a simple cylinder of approximately 4' diameter containing an internal bulkhead T-butt welded to the shell, and closed at both ends by hemispherical domes. The forward dome incorporated an access hatch.

The vessel was subjected to an external pressure cycle in a pressure chamber using the soft cycling principle in which water is introduced into the chamber and maintained at a constant pressure. The vessel is then filled with water to the same pressure and then alternately depressurised and pressurised, thus producing an externally applied compressive load to the vessel. Cracking occurred at the toe of the T-butt weld. Fig. 3 shows a cross section of the T-butt weld, illustrating the fatigue cracking.

Crack initiation and propagation were obtained using the following NDE techniques.

AMLEC (Eddy Current) (1)

This was used principally to detect the onset of cracking. Measurements were made inside the vessel, i.e. the model was drained down, a technician entered the vessel through the small access hatch and took readings with the vessel still in the pressure chamber.

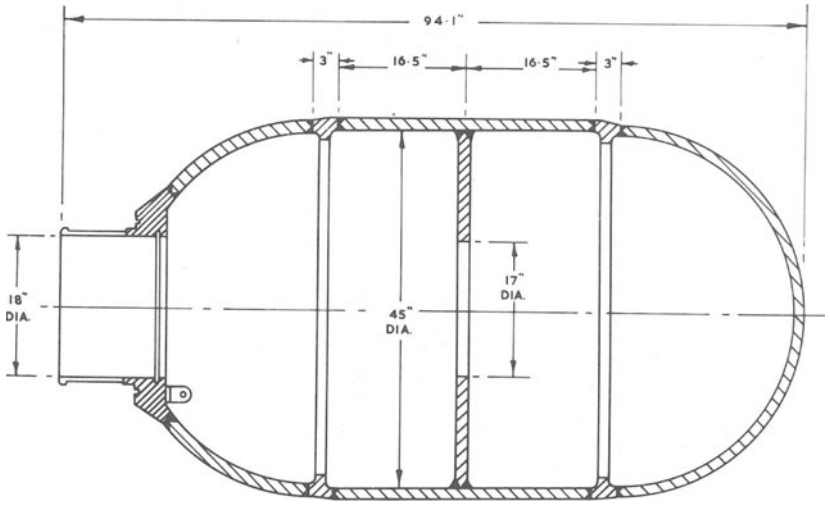

Fig. 2. Fatigue Test Vessel - S8/1.

ACPD (1) (2)

Cracks located by AMLEC were sized using this technique - again operating inside the vessel.

Ultrasonic Diffraction (1)

Like ACPD this is a crack sizing technique and was used to establish the final crack profile on completion of the fatigue test. Crack sizing was done outside the vessel after extraction from the pressure chamber.

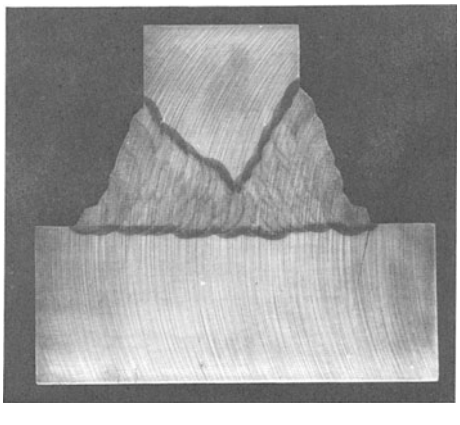

Fig. 3. Fatigue Crack at Forward Toe of T-butt Weld.

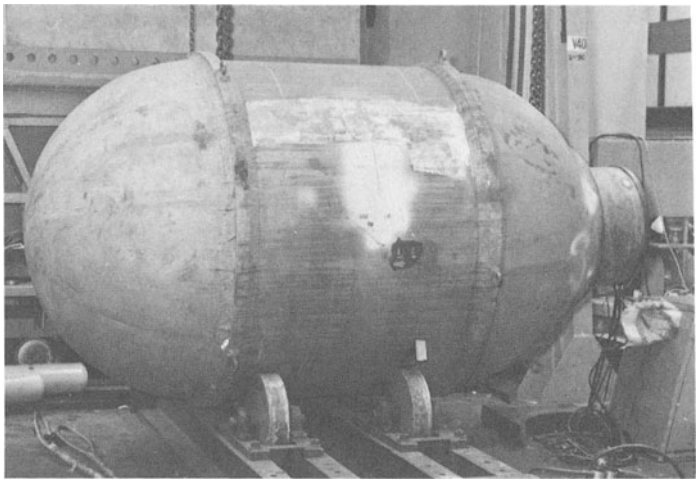

Fig. 4. Through Shell Fatigue Crack in Vessel S8/1.

CONDUCT OF FATIGUE TEST

Fatigue cycling was carried out in approximately 2,000 cycle stages with a break for NDE at the end of each stage. The vessel failed at 46,500 cycles sustaining a through shell crack about 4 inches long emanating from the forward T-butt weld toe, Fig. 4.

CONDUCT OF NDE

Before cycling the vessel, a base line survey was carried out in which AMLEC and ACPD measurements were taken at 5^{o} intervals round the circumference at both forward and aft toes of the bulkhead to shell T-butt weld i.e. 72 measurement stations. These measurements were repeated at the end of each 2,000 cycle stage right up to final failure. During the course of the test approximately 24 measurements at each of the 72 stations were made with ACPD, (somewhat less for AMLEC), i.e. just over 1700 data points for both forward and aft weld toes.

In the event very little cracking occurred at the aft toe so that all the following data refer to the forward toe position.

ANALYSIS OF RESULTS

The ACPD crack length (a) and AMLEC readings were plotted against the number of fatigue cycles (N) for each of the 72 measurement stations. The AMLEC plots were used to establish, for each station, the number of cycles corresponding to zero cracking. Fig. 5 shows a typical plot showing that for this station (10^{o}) zero cracking was at 10,000 cycles.

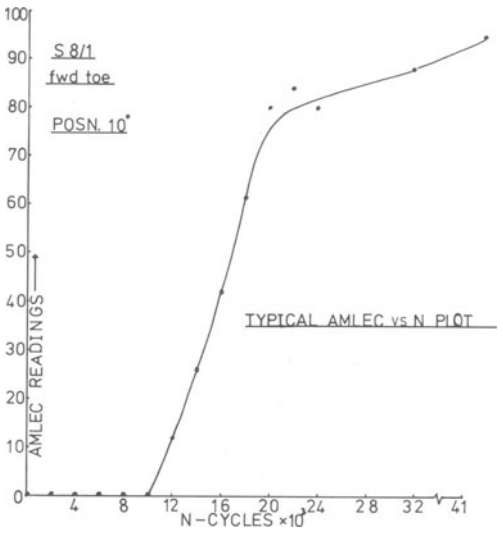

Fig. 5. Typical Eddy Current/Fatigue Cycles Plot.

Fig. 6 shows a typical ACPD crack length vs N plot again for the 10^{o} station. As can be seen the first indication of cracking was at 12,000 cycles. Zero cracking was taken as indicated by AMLEC at 10,000 cycles. A best fit curve was then drawn through the plotted ACPD points. This procedure was repeated for all ACPD measurement stations to yield best fit curves for all 72 stations.

The curve in Fig. 6 is typical of all the plots showing an initial acceleration of crack growth followed by a sensibly straight line portion, then at deeper crack lengths a decrease in growth rate. The main differences between curves at each station were:

(a) the number of cycles to initiation.

(b) the duration of the straight line portion and consequently the crack depth at which growth rate tailed off.

In no case was there an ACPD indication of the presence of a crack at less than 12,000 cycles and similarly in no case did AMLEC indicate zero cracking at less than 10,000 cycles. It was therefore concluded that the earliest detectable initiation had occurred at 12,000 cycles.

In order to get a picture of the development of initiation sites round the circumference at the forward toe of the bulkhead to shell T-butt weld a polar plot of crack length against number of cycles was constructed using values taken from the best fit curve

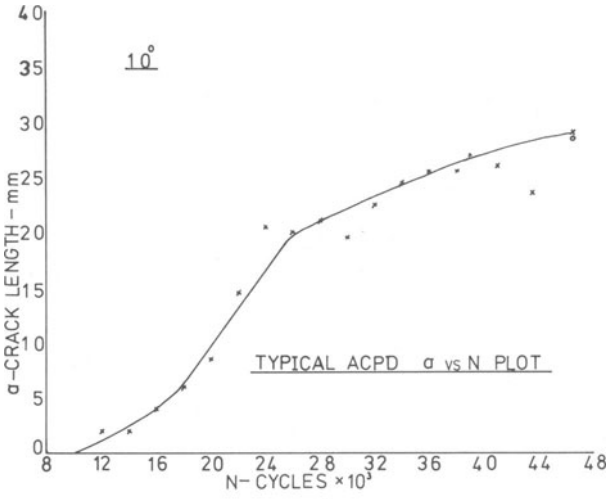

Fig. 6. Typical ACPD Crack Length/Fatigue Cycles Plot.

for each measurement station. The result is shown in Fig. 7. The circumference represents the toe of the weld while the radial axis represent the shell thickness. The figure shows that initiation occurred at several sites around the circumference and that initiation at these sites did not occur simultaneously. Initiation first occurred at 12,000 cycles at four sites; by 14,000 cycles another three sites appeared; by 16,000 cycles another one site; by 18,000 cycles six additional sites appeared and by 20,000 cycles another two sites became active. At the next measurement stage of 22,000 cycles a full circumferential crack of varying depth had developed, indicating of course that all the initiation sites had been developing in both the radial and circumferential directions to coalesce at approximately 22,000 cycles.

Fig. 8 shows the development of the full circumferential crack from 22,000 cycles to final failure at 46,500 cycles. Again these polar plots were constructed from the ACPD crack length vs number of cycles best fit curves referred to earlier. For clarity, the results have been plotted at 4,000 cycle intervals (instead of the actual 2,000 cycle intervals).

As can be seen the crack finally grew to a through crack at $270/275^{o}$. It is interesting to note that the shell is made in two halves which are joined by longitudinal seam welds at approximately 270^{o} and 90^{o}. Thus, it will be seen that the through crack occurred where the 270^{o} longitudinal seam weld crossed the circumferential bulkhead to shell T-butt weld.

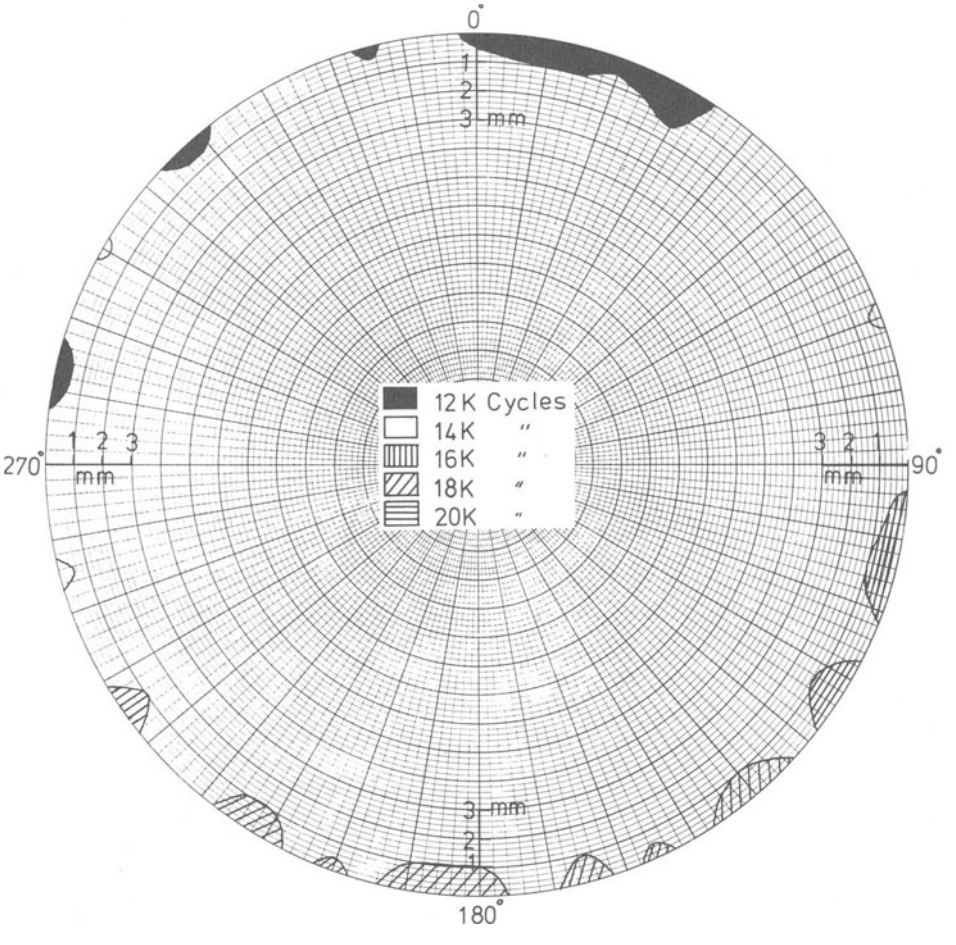

Fig. 7. Development of Crack Initiation Sites in Vessel S8/1, (Crack Lengths Measured by ACPD).

It can also be seen from Fig. 8 that the fatigue crack at the position of the other crossing weld, i.e. the 90° longitudinal seam, consistently lags behind as cycling proceeds. The reason for this behaviour is not known at the present time.

Referring again to Fig. 4, which shows the through crack indicated by magnetic particle examination. The magnetic particle indicated through cracking over a greater distance than actually was through, this is due to the fact that the crack tip is just sub-surface as indicated by Fig. 9 which shows the crack at 265° to be almost through. In fact plasticity at the crack tip can be seen indicating that it was on the point of shearing through. Fig. 10

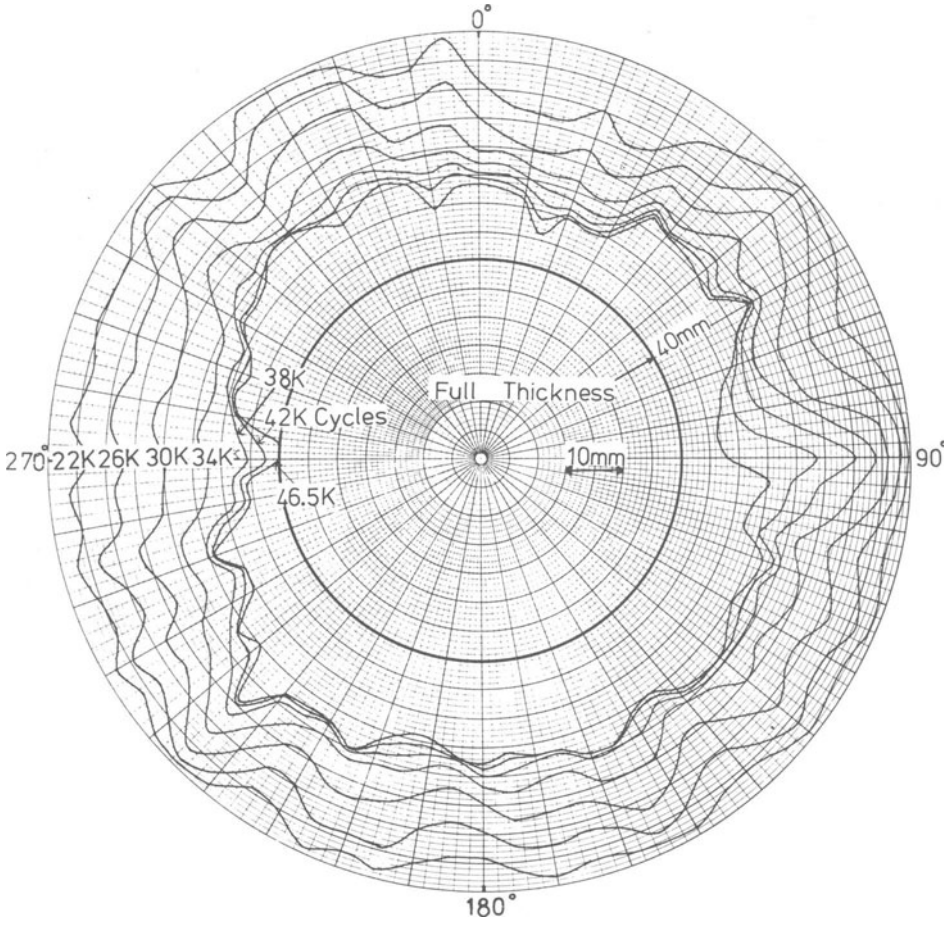

Fig. 8. Propagation From Full Circumferential Crack to Through Shell Crack in Vessel S8/1.

shows the through crack at 270°, and also illustrates very nicely the crossing longitudinal seam weld.

Fig. 11 is again plotted in polar form and shows the final circumferential crack depth profile as measured by ACPD and ultrasonic diffraction together with the actual depth profile obtained by sectioning and optical measurement.

The full line is the actual profile, the dashed is ACPD, and the dotted ultrasonic diffraction.

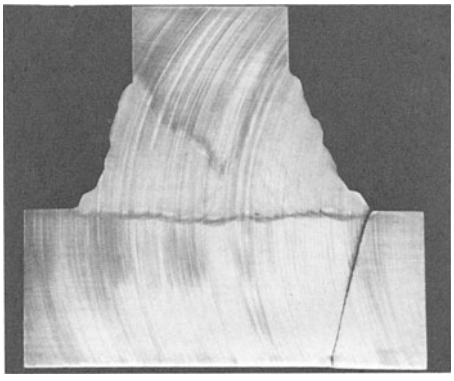

Fig. 9 Fatigue Crack at 265° Position - Vessel S8/1.

The ACPD is reasonably good although in certain parts it grossly underestimates the crack size, e.g. at 35° and 225° the readings are about 40% low. The reasons for such wide discrepancies are being investigated but it is suspected that it may be due to crack closure, inclusions or crack branching, etc. There is of course the chance of operator error in the cramped conditions under which these measurements were taken inside the vessel.

The ultrasonic diffraction is in excellent agreement with the actual profile.

The actual vs ACPD or ultrasonic measurement in terms of percentage error is shown in Fig. 12. The vertical axis is the percentage of the total number of measurements made falling within each percentage error band on the horizontal axis. From this it can be seen that for ACPD about 70% of the results are within $\pm$15% of the actual crack size while for ultrasonic diffraction we have

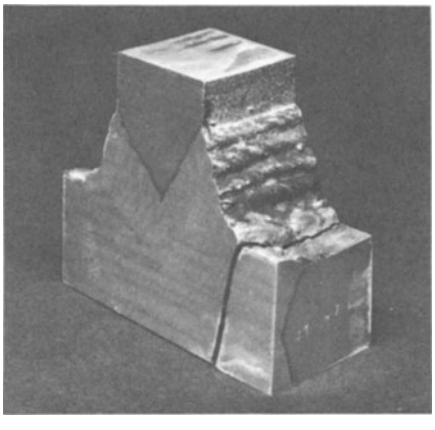

Fig. 10. Through Crack at 270° Position - Vessel S8/1. Also shows Crossing Longitudinal Seam Weld.

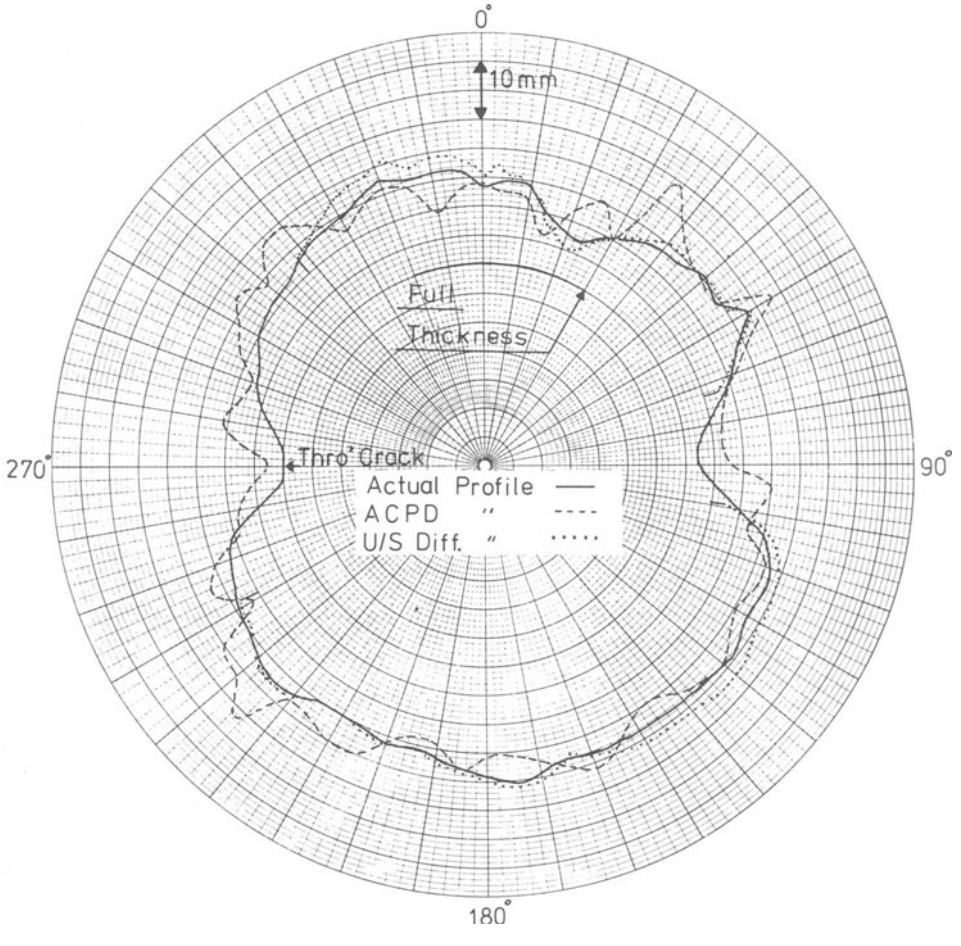

Fig. 11. Final Crack Profile, Forward Toe Bulkhead T-butt Weld in Vessel S8/1 at 46.5K Cycles.

95% of the results within $\pm$10%. In fact we have almost 40% of the results within $\pm$2.5%.

COMPARISON OF EXPERIMENTALLY DETERMINED CRACK GROWTH RATES WITH THEORETICAL FRACTURE MECHANICS FATIGUE ANALYSIS

Fig. 13 shows the results of plotting all the ACPD measured crack lengths for all positions i.e. 0-355° from a common initiation point defined as a_o = 2 mm. By doing this the very long initiation lives of many of the positions is eliminated. This was done to illustrate that the crack propagation rate is basically similar at all positions over the nearly linear portion of the curve. The very

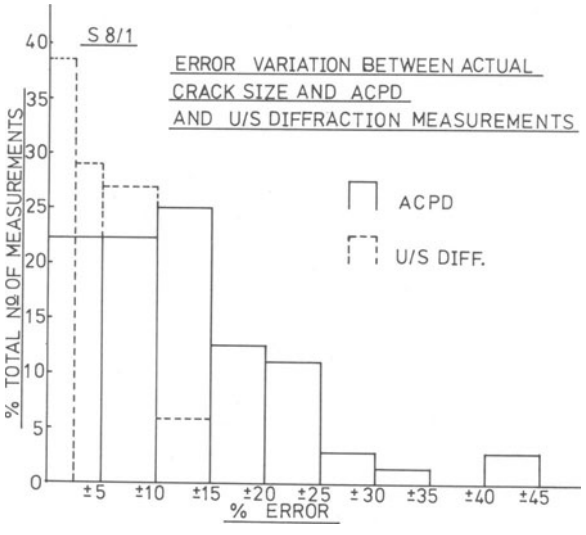

Fig. 12. ACPD and Ultrasonic Diffraction Percentage Errors on Final Crack Depths.

wide spread from about 16,000 cycles on is of course due to the fact that most positions did not crack right through, and reflects the range of final crack sizes.

For the comparison of theory with experiment the ACPD results at 270^{o} and 275^{o} were plotted and a best fit curve drawn through them, Fig. 14. These were the positions over which the crack had

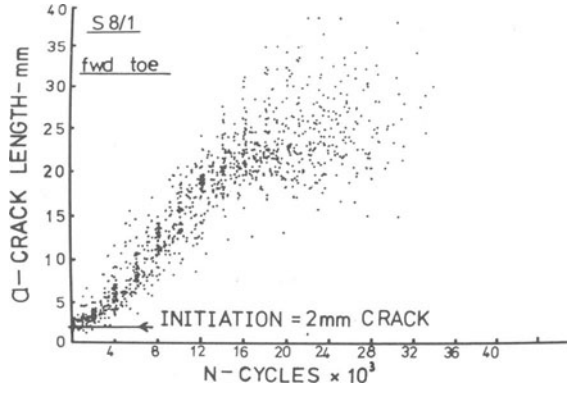

Fig. 13. ACPD Crack Length versus Cycles for All Stations 0^{o}-355^{o}.

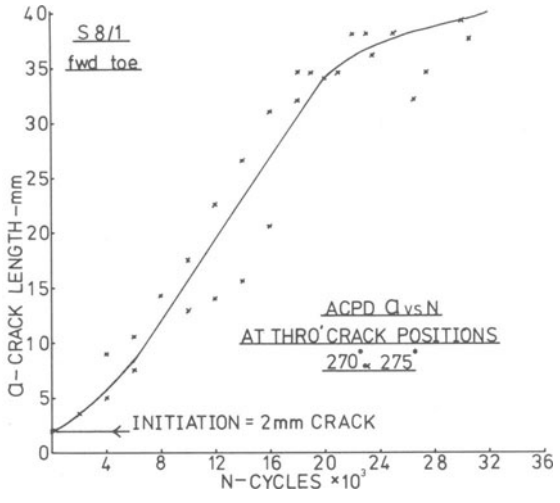

Fig. 14. ACPD Crack Length versus Cycles - 270° and 275°.

fully penetrated the shell. Again an initial crack size of 2 mm was assumed so that only the propagation phase is considered.

From a knowledge of the applied loading, restraint stress measurements and fatigue crack growth rate data in terms of the applied stress intensity range it was possible to make a fracture

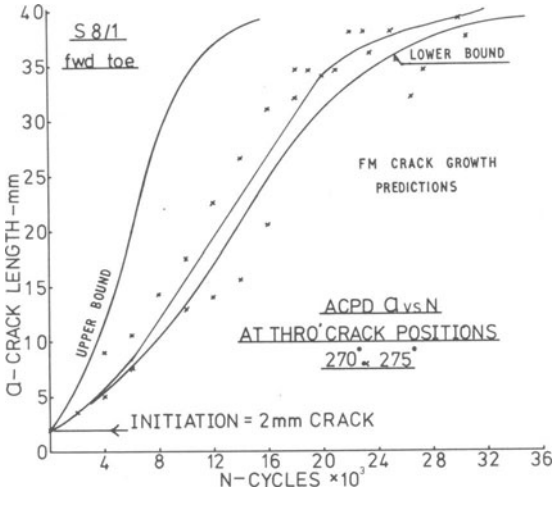

Fig. 15. Comparison of Upper and Lower Bound Fracture Mechanics Predicted Growth Behaviour With Experimental Data.

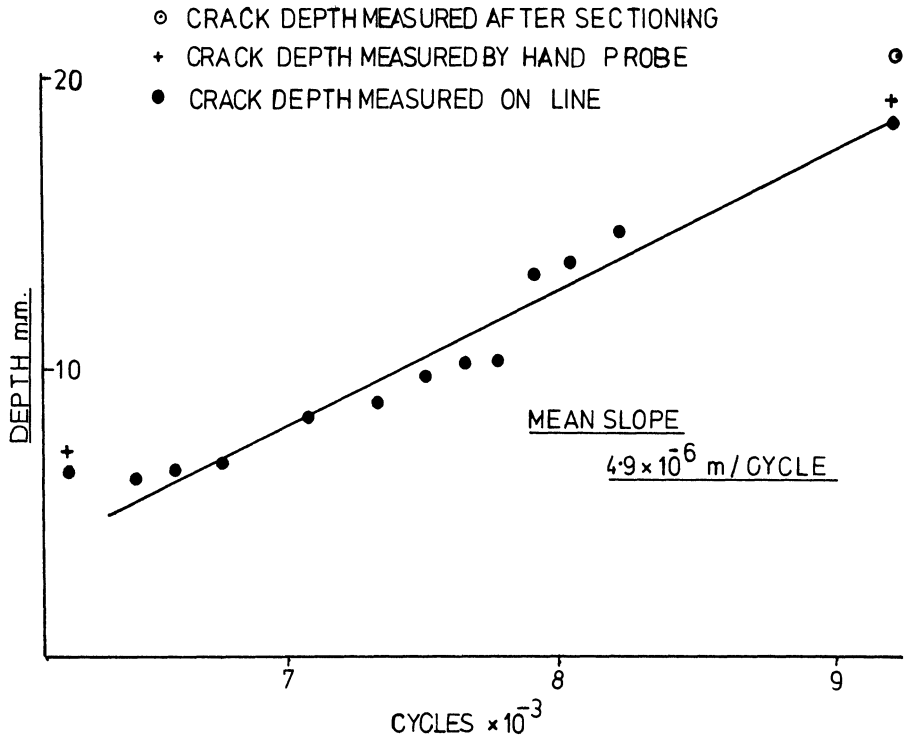

Fig. 16. On-Line ACPD Crack Depth versus Cycles Plot.

mechanics prediction of crack depth versus number of cycles. Fig. 15 shows the derived upper and lower bound curves superimposed on the experimental curve. From this it can be seen that our theoretical model predicts the growth rate behaviour fairly satisfactorily.

Details of the fracture mechanics fatigue analysis appear in Annex A.

ON-LINE UNDERWATER ACPD MEASUREMENT

As mentioned earlier the vessels are fatigued in the pressure chamber using the soft cycling principle. Thus the on-line ACPD had to operate underwater at fluctuating water pressures of several thousand psi.

Fig. 16 shows the encouraging results obtained, the ACPD depth is within 2 mm of the true depth and the difference between on-line and hand probe results was less than 1 mm, (NB. These results were obtained on a different design vessel from S8/1 referred to above).

Full details of the on-line work are given in Annex B.

CONCLUSIONS

1. Non-destructive techniques applied to fatigue crack detection and monitoring have been shown to be very useful tools in providing the essential data required for a fracture mechanics fatigue analysis of a compressively fatigue loaded welded pressure vessel.

2. The eddy current technique proved to be a reliable indicator of crack initiation which occurred at the forward toe of the stiffener to shell T-butt weld.

3. ACPD and eddy current indicated non-simultaneous multiple crack initiation with a spread of initiation lives ranging between 12,000 and 20,000 cycles. A full circumferential crack was indicated by ACPD at 22,000 cycles.

4. Crack sizing by hand probe ACPD has been successfully used to monitor fatigue crack propagation.

5. On-line underwater ACPD shows promise as a continuous crack monitoring technique.

6. A comparison of final crack depth profile, measured by sectioning, with ACPD and ultrasonic diffraction measured profiles indicated that 70% of the ACPD results were within $\pm$15% and 95% of the diffraction results were within $\pm$10% of the actual depth. In fact 40% of the diffraction measurements were within $\pm$2.5%.

7. ACPD indicated that propagation rate was similar at all measurement stations.

8. A theoretical fracture mechanics fatigue analysis gave good agreement with the experimentally ACPD determined crack propagation at the through shell crack positions.

REFERENCES

1. I.M. Kilpatrick and J.M. Cargill, "Fatigue Crack Detection and Sizing in Welded Steel Structures", DARPA/AFML Review of Progress in Quantitative NDE, 1980.
2. W.D. Dover, F.D.W. Charlesworth, K.A. Taylor, R. Collins and D.H. Michael, "The Use of A.C. Field Measurements to Determine the Shape and Size of a Crack in a Metal", in: "Eddy Current Characterisation of Materials and Structures", G. Birnam and G. Free, eds., ASTM STP 722, 1981.

3. J.D.G. Sumpter and A.R. Morris, "Elastic Stress Intensity Factors for Fatigue Analysis of Framed Cylinders", Unpublished AMTE Report, 1981.
4. L.A. Pipes, "Applied Mathematics for Engineers and Physicists", McGraw Hill, 1958.
5. P. Moon and D.E. Spencer, "Field Theory for Engineers", Van Nostrand.